

Investigation of major parameters affecting instability of steel beams with RBS moment connections

A. Moslehi Tabar[†] and A. Deylami[‡]

*Department of Civil Engineering, Amirkabir University of Technology,
P. O. Box 15815-3537, Tehran, Iran*

(Received January 20, 2005, Accepted January 4, 2006)

Abstract. One of the most promising ways through which a steel moment frame may attain high energy dissipating capability is to trim off a portion of the beam flanges near the column face. This type of moment connection, known as Reduced Beam Section (RBS) connection, has notable superiority in comparison with other moment connection types. As the result of the advantages of RBS moment connection, it has widely being used in practice. In spite of the good hysteretic behaviour, an RBS beam suffers from an undesirable drawback, which is local and lateral instability of the beam. The instability in the RBS beam reduces beam load-carrying capacity. This paper aims to investigate key issues influencing cyclic behaviour of RBS beams. To this end, a numerical analysis was conducted on a series of steel subassemblies with various geometric properties. The obtained results together with the existing experimental data are used to study the instability of RBS beams. A new slenderness concept is presented to control an RBS beam for combined local and lateral instability. This concept is in good agreement with the numerical and experimental results. Finally, a model is developed for the prediction of the magnitude of moment degradation owing to the instability of an RBS beam.

Keywords: steel structures; RBS moment connection; panel zone; instability; cyclic loading; ductility.

1. Introduction

The 1994 Northridge and 1995 Kobe earthquakes caused unprecedented damages to the conventional welded beam-to-column connections. Brittle fracture within weldments connecting beam flange to column face or within heat affected zones was the main type of defects detected after those earthquakes. Some experimental studies before and after the earthquakes also revealed the inherent drawbacks of the conventional welded moment connections (Engelhardt and Husain 1993, Miller 1998, Mahin 1998, and Calado 2000). Since the 1994 Northridge earthquake, a variety of investigations have been carried out in order to find solutions to these deficiencies (SAC 1995).

The efforts made to improve cyclic behaviour of the conventional moment connections have resulted in two general modification methodologies. The more traditional one is to stiffen the moment connections. This is accomplished by adding cover plates, haunches and vertical ribs, etc. to the connection. The latest alternative modification approach is to soften a portion of beam flanges near the column face (Plumier 1997). Among various methods to soften a connection, the Reduced Beam

[†]Ph.D. Candidate

[‡]Professor, Corresponding author, E-mail: deylamia@aut.ac.ir

Section moment connection with circular cut is worthy to note. Even though these two methodologies are entirely different in appearance, they both trace a common goal, i.e.: to lead plastic hinges to a location within the beam span away from column face, resulting in reduction of stress concentration at the interface of beam and column.

Extensive experimental studies have confirmed that RBS moment connection is one of the most cost-effective ways to improve seismic behaviour of the conventional moment connections (Engelhardt *et al.* 1996, 1998, Yu *et al.* 1999, and Yu and Uang 2001). This type of moment connection can develop a high level of ductility. That is why this connection type has widely being used in practice. Despite of the fact that the RBS connection is able to dissipate a large amount of energy, there is a major problem with this connection type that is reduction of load-carrying capacity owing to the instability of beam. Some studies have been conducted to assess the key issues influencing the instability of RBS beams (Uang and Fan 1999, Yu *et al.* 1999, Uang and Fan 2001, and Yu and Uang 2001). The local and lateral slenderness ratios were the parameters which first drew attention of researchers because reducing the beam flange section degrades the restraint against local and global out-of-plane deformations. Uang and Fan (1999, 2001) performed a valuable comprehensive statistical analysis upon a series of laboratory results. They stated that the cyclic behaviour of RBS beams is predominantly affected by the web local buckling.

Another factor, which can influence failure mode of the beams with RBS moment connections, is column panel zone (PZ) strength. Krawinkler (1978), Popov (1987) and El-Tawil *et al.* (1999) indicated that the beam-to-column joints with weak PZ encounter high shear deformation, resulting in brittle fracture within weldment connecting beam flange to column face. As a result, in spite of weak PZ ability in dissipating a large amount of energy, using very weak joints is not recommended. On the contrary, in the presence of strong PZ, fracture potential is reduced, but the possibility for beam instability rises, especially for RBS connections. Tsai and Chen (2000) and Jones *et al.* (2002) experimentally illustrated that moderately strong PZs show appropriate performance.

The objective of this paper is to develop a model as an index to control the instability of RBS beams. A numerical analysis was conducted on a series of steel subassemblies with various geometric properties. The results verify that partial shear yielding in PZ can improve hysteretic behaviour of specimens by avoiding premature instability in the beams. Furthermore, a new slenderness concept is expressed to check an RBS beam for the combined local and lateral instability. The effects of the beam web and lateral slenderness as well as the effect of PZ ductility are addressed in this model. In addition, a mathematical model is derived for prediction of the magnitude of beam moment deterioration in terms of the proposed slenderness parameter. The model agrees with the obtained numerical results and with the existing experimental data.

2. Parametric study

A parametric study was conducted to investigate local and lateral instability of RBS beams with an emphasis of the effect of PZ properties. Nine subassemblies with the general configuration shown in Fig. 1(a) were considered. The column was supported at the base by a hinge, while a vertical roller was used at another end. The beam was laterally braced at a distance of 150 cm from the column face. This distance coincides with AISC *Seismic provisions* (2002). The design of these models is described in the next section.

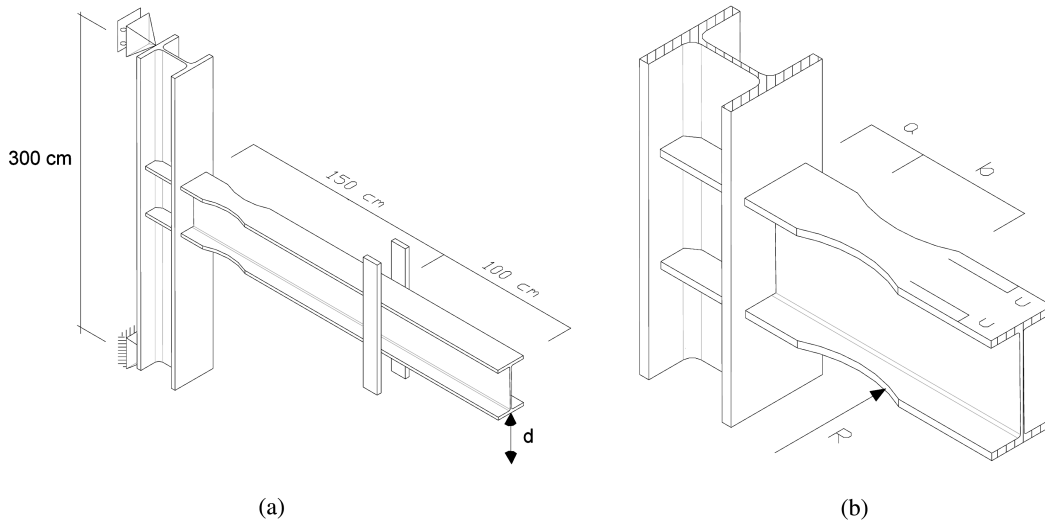


Fig. 1 Configuration of (a) subassembly; (b) RBS connection

2.1. Specifications of models

This study is directed along the authors' previous paper (Deylami and Moslehi Tabar 2004). Two groups of models, designated by RBS1 and RBS2, were investigated by Deylami and Moslehi Tabar (2004). The first group, RBS1, consisted of an IPE300 beam and an IPB200 column. The second group of models, RBS2, was made up of IPE450 for beam and IPB300 for column. In the present paper another set of models is involved. In this set, designated by RBS3, an IPE600 beam is framed to an IPB400 column. The beams and columns were pre-selected so that they could produce weak column panel zones at the intersection of beam and column. Then, for evaluating the effect of PZ thickness, in each set of models, RBS1, RBS2 and RBS3, column panel zone was reinforced by a 6 mm and a 10 mm thick doubler plate in order to provide balanced and strong PZ, respectively.

2.2. PZ strength

In order to judge how strong PZ is, the design shear demand, V_r , was compared with the ultimate shear strength of column panel zone, V_y , as recommended by AISC *Seismic provisions* (2002). They both can be computed as follows:

$$V_y = 0.6F_y d_c t_{pz} (1 + 3 b_{cf} t_{cf}^2 / d_b d_c t_{pz}) \quad (1)$$

$$V_r = \beta_E M_p \left[\frac{1}{0.95 d_b} - \frac{L_b + d_c / 2}{L_b} \cdot \frac{1}{H} \right] \quad (2)$$

in which F_y = yield stress of PZ material; M_p = plastic moment capacity of beam section; L_b = beam length from column face to beam tip; and H = column height. d_c , d_b , d_{cf} , t_{pz} , and t_{cf} are column depth, beam depth, column flange width, PZ thickness, and column flange thickness, respectively. In Eq. (2), $\beta_E M_p$ is the flexural demand imposed at the column face. It is suggested that β_E is limited between 0.85 and 1 (Engelhardt *et al.* 1998). $\beta_E = 0.85$ was taken as an initial assumption.

Table 1 Specifications of models

Spec.	Col.	Beam	Doubler Pl. th. (mm)	V_r/V_y
RBS1-W	IPB200	IPE300	0	1.20
RBS1-B	IPB200	IPE300	6	0.78
RBS1-S	IPB200	IPE300	10	0.63
RBS2-W	IPB300	IPE450	0	1.14
RBS2-B	IPB300	IPE450	6	0.78
RBS2-S	IPB300	IPE450	10	0.65
RBS3-W	IPB400	IPE600	0	1.06
RBS3-B	IPB400	IPE600	6	0.77
RBS3-S	IPB400	IPE600	10	0.65

Characteristics of the models as well as their ultimate shear strength and design shear demand are given in Table 1. In this study, the PZs without doubler plate are known as weak panels. The relatively thick PZs, whose ultimate shear strength is notably more than the design shear demand, are designated as strong panels. The balanced panel zones lie between two aforementioned limits. Accordingly, each set of models consists of weak, balanced, and strong PZs, which are designated, respectively, by letters W, B, and S in Table 1.

2.3. Strong column-weak beam criterion

According to AISC *Seismic provisions* (2002), the following relationship must be satisfied at beam-to-column connections:

$$\frac{\sum M_{pc}^*}{\sum M_{pb}^*} > 1.0 \quad (3)$$

where

$\sum M_{pc}^*$ = the sum of the moments in the column above and below the joint at the intersection of the beam and column centerlines. It is permitted to take $\sum M_{pc}^* = \sum Z_c (F_{yc} - P_{uc}/A_g)$, in which A_g , F_{yc} , P_{uc} , and Z_c are, respectively, gross area of column, column yield strength, required column axial compressive strength, and plastic section modulus of column.

$\sum M_{pb}^*$ = the sum of the moment(s) in the beam(s) at the intersection of the beam and column centerlines. When RBS connection is used, it is permitted to take $\sum M_{pb}^* = \sum (1.1R_y F_y z + M_v)$, where z is the minimum plastic section modulus in the RBS region, and R_y is ratio of the expected yield strength of the beam to the minimum specified yield strength. R_y shall be taken as 1.5 for A36 steel. M_v is the additional moment due to shear amplification from the location of the plastic hinge to the column centerline. Based on the configuration shown in Fig. 1, M_v is assumed to be $1.1R_y F_y z \frac{d_c/2 + a + b/2}{L_b - a - b/2}$.

Estimating the required column axial compressive strength, P_{uc} , as $1.1R_y F_y z / (L_b - a - b/2)$, the ratio $\sum M_{pc}^* / \sum M_{pb}^*$ for all the models will be as the values given in Table 2.

Table 2 Column-beam moment ratios

Spec.	$\sum M_{pc}^*$	$\sum M_{pb}^*$	$\sum M_{pc}^* / \sum M_{pb}^*$
RBS1	304.5	186.1	1.64
RBS2	872.4	518.4	1.68
RBS3	1499.8	1106.7	1.35

Table 3 RBS region dimensions

Beam	a (mm)	b (mm)	c (mm)	b_f^{rbs*} (mm)	R (mm)
IPE300	80	200	32	86	172.25
IPE450	120	350	45	100	385.28
IPE600	140	400	55	110	391.13

* b_f^{rbs} = the minimum width of beam flange within the RBS region

2.4. Design of RBS region

The radius cut as shown in Fig. 1(b) was employed for the RBS region. The RBS connections were designed according to the recommendations proposed by Engelhardt *et al.* (1998). Resulting dimensions for the RBS region are noted in Table 3.

3. Finite element analysis

3.1. Modeling and analysis

The ANSYS finite element software (1992) was utilized to model the specimens for large-deformation nonlinear analysis. The analyses were primarily intended to investigate the overall cyclic behaviour of the subassemblies with an emphasis on the influence of PZ properties. The subassemblies were modeled using a quadrilateral 4-node shell element (element SHELL43 in ANSYS) with possibility to employ material nonlinearity. SHELL43 has plasticity, large deflection, and large strain capability. It has six degrees of freedom per each node: translations in the x , y , z directions, and rotations about x , y , z axes. Fig. 2 shows a typical finite element meshing used in this study. As observed in Fig. 2, a more refined mesh was applied for the regions near the RBS. Since it was expected that nonlinear deformations were mostly accommodated around the beam-to-column joint, nonlinear material was assigned to the elements within those portions. For the remaining parts of the models, the material was assumed to behave elastically. The plasticity model was based on the von Mises yielding criteria and its associated flow rule. The fundamental assumptions made to idealize steel mechanical properties were included: Young's modulus = 210 GPa, Poisson's ratio = 0.3, yield stress = 250 MPa, ultimate tensile strength = 370 MPa, and tangent modulus = Young's modulus / 100.

In order to verify the validity of this numerical research, Deylami and Moslehi Tabar (2004) prepared a finite element model for the specimen DB3 of the experimental study conducted by Engelhardt *et al.* (1998). This model was analyzed under cyclic displacement control loading using ANSYS finite element software (1992). The moment-total plastic rotation hysteretic response resulted from this

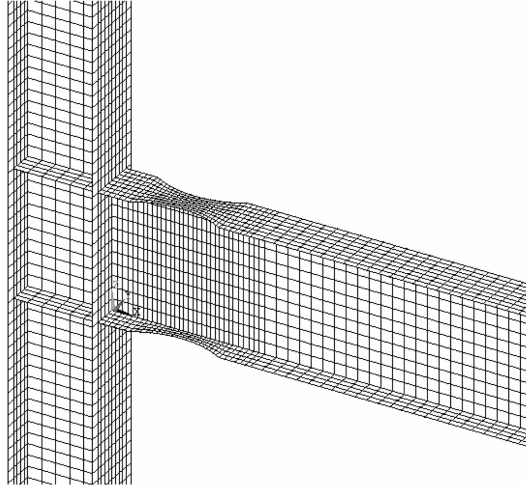


Fig. 2 Three dimensional finite element model

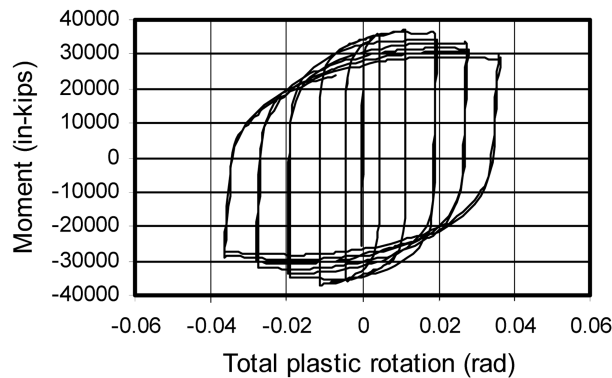


Fig. 3 Analytical hysteretic response of specimen DB3

analysis is shown in Fig. 3. The numerical results suitably agreed with the experimental data. Three key parameters were taken as the base of comparison: (1) the maximum moment developed at the column face: the difference between the maximum moments at the column face resulted from the two studies is less than 4%; (2) the onset of flexural moment deterioration: in the both studies, the moment-rotation loops initiate to deteriorate after a plastic rotation of 0.02 radians; and (3) the total reduction of the maximum moment at the column face: the total reduction of the moment at the end of loading is about 22% for numerical analysis and about 28% for the test.

3.2. Loading procedure

Each subassembly was loaded on its beam tip by imposing cyclic displacement according to the SAC loading protocol (Clark *et al.* 1997). Cyclic nonlinear analyses of the subassemblies were performed using Riks method. In this method, buckling mode shapes of the model, computed in a separate

buckling analysis, are implemented to perturb the original perfect geometry of the model. Then, the obtained imperfect model is analyzed to take local and lateral buckling into account.

4. Analysis results

4.1. Hysteretic response

Moment-total plastic rotation hysteretic response of the subassemblies resulted from the finite element analyses are shown in Fig. 4. The beam moment was measured at the column face, and the rotation was computed by dividing the total plastic beam tip deflection by the beam length.

In the models with weak PZ, RBS1-W, RBS2-W, and RBS3-W, no significant reduction is observed in the beam moment capacity. They showed, indeed, expanding and stable hysteretic behaviour. The panel zones underwent high inelastic shear deformation and thoroughly yielded. In these models, the PZs played a main role in the energy dissipation. However, according to the investigation performed on the stress state at the interface of the tension beam flange and column face (Deylami and Moslehi Tabar 2004), it can be concluded that although models with weak PZ reveals stable hysteretic response, the beam-to-column connections are strongly susceptible to fracture at the conjunction of beam flange and column face before attaining the required plastic rotation.

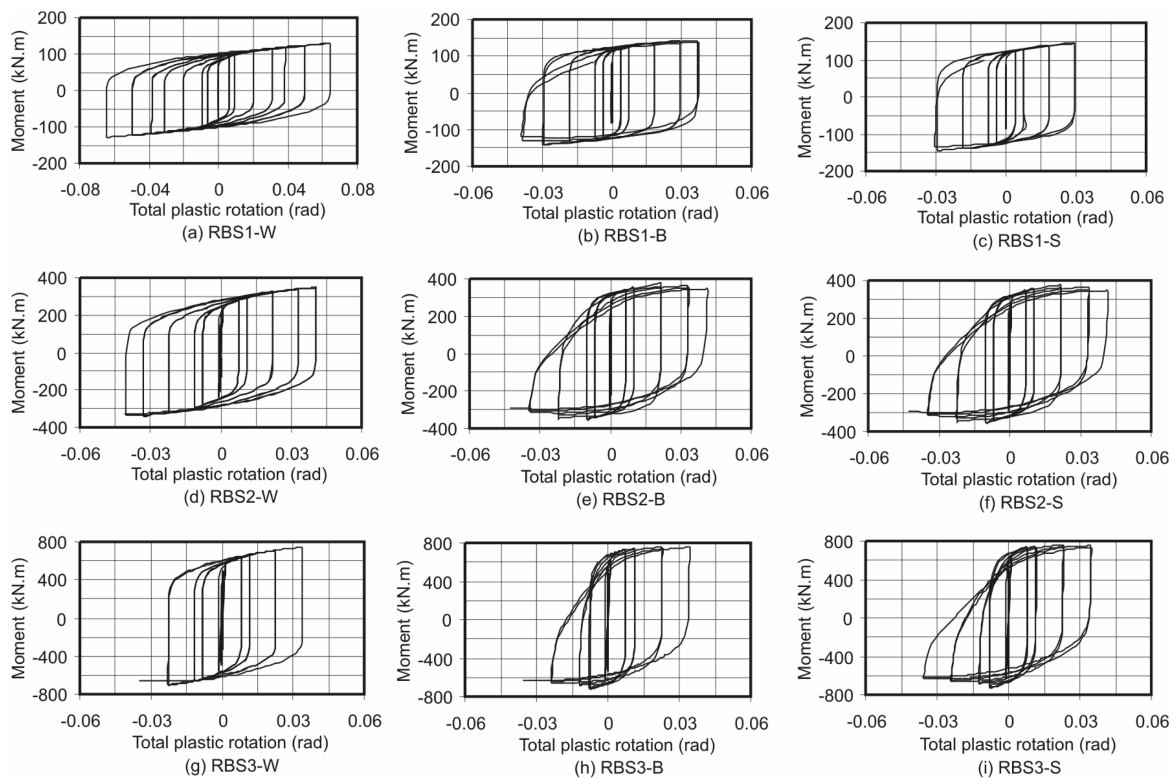


Fig. 4 Hysteretic response of the models

In the models with strong PZ, the lateral and local buckling reduced the flexural moment capacity of beam. The moment capacity reduction depends on the buckling mode which predominantly influences cyclic behaviour of model. For instance, in the model RBS1-S, which possesses relatively slender beam and more compact web, lateral-torsional buckling dominated hysteretic behaviour. Indeed, the secondary tensile stress arisen from the out-of-plane deformations was added to the tensile stress due to in-plane stress. As a result, before a significant reduction took place in the beam moment capacity, approximately uni-axial stress within the RBS region had exceeded the ultimate tensile strength of steel material, and the cyclic loading was therefore stopped. On the contrary, the local web buckling became a remarkable concern in the models RBS2-S and RBS3-S. In this case, load-carrying capacity of the models gradually deteriorated until the uni-axial stress in the RBS reached the ultimate tensile strength. The gradual deterioration of load-carrying capacity in the latter case arises from less out-of-plane deformations and less secondary tensile stress caused by lateral buckling. Uang and Fan (1999, 2001) have indicated in their valuable research that the web local buckling is the most important buckling mode in RBS beams. However, according to this study, it seems the lateral buckling may be more detrimental than the web local buckling, especially for laterally slender beams.

The balanced PZ models had the same cyclic behaviour as the strong PZ ones. In these subassemblies, the PZs properly participated with the RBS moment connections in energy dissipation. It denotes that using a moderately thick doubler plate reduces the maximum moment developed at the column face. In Fig. 5, the amount of energy dissipated by PZ (%) at a plastic rotation of 0.03 radians is depicted in

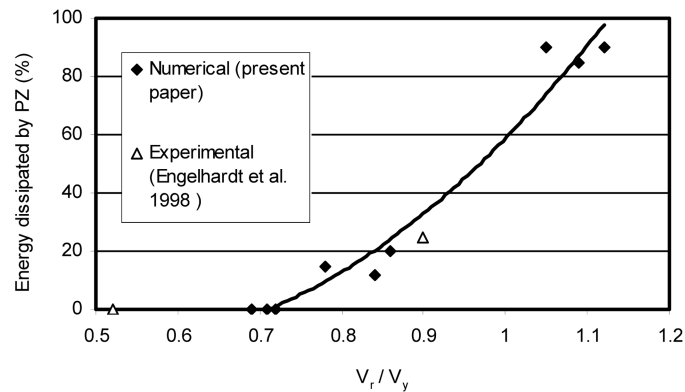


Fig. 5 Effect of PZ shear strength on amount of PZ energy dissipation

Table 4 Real magnitudes of the coefficient β_E

Spec.	V_r (kN)	V_{\max} (kN)	β_E
RBS1-W	404.6	367	0.80
RBS1-B	404.6	447	0.94
RBS1-S	404.6	459	0.96
RBS2-W	685.5	675	0.84
RBS2-B	685.5	735	0.91
RBS2-S	685.5	747	0.93
RBS3-W	1000.8	990	0.84
RBS3-B	1000.8	1020	0.87
RBS3-S	1000.8	1060	0.90

terms of the ratio V_r/V_y . The figure expresses that for V_r/V_y smaller than 0.7, PZ is not expected to share with RBS region in energy dissipating.

For each model, the real magnitude of the coefficient β_E , which had been formerly assumed to be 0.85, is given in Table 4. To obtain the coefficient β_E for the models, the maximum moment developed at the column face were divided by the plastic moment capacity of the beam section, M_p . It should be noted that V_{\max} is the maximum shearing force imposed on PZ. Table 4 shows that the coefficient β_E varies in the range of 0.80 to 0.96. Consequently, $\beta_E = 0.85$ may be a rational initial assumption.

5. Analysis of beam instability

The lateral instability combined with the web and flange local buckling modes are the sources of the instability in RBS beams. Laboratory observations (Yu *et al.* 1999) and numerical results indicate that various buckling modes generally do interact with each other. Accordingly, in the following, after studying the influence of each buckling mode separately, the interaction between the local and lateral buckling modes is analyzed. The obtained numerical results and preceding experimental data (Engelhardt *et al.* 1998, Popov *et al.* 1998, Yu *et al.* 1999, and Chi and Uang 2002) are brought together to reach a more reliable conclusion.

5.1. Lateral instability

The resistance of flexural members to lateral-torsional buckling is conventionally evaluated by the lateral slenderness ratio, i.e., L_0/r_y . The parameter L_0 is laterally unsupported length of beam, and r_y equals to the beam radius of gyration about the minor axis. However, in RBS beams, as a result of the variation in the mechanical and cross-sectional properties, definition of such a ratio becomes more complicated. Uang and Fan (1999, 2001) have used two slenderness parameters for RBS beams as $\bar{\lambda}_{LTB} = (L_0/r_y)/\lambda_{LTB}$ and $\bar{\lambda}_{LTB}^{rbs} = (L_0/r_{y\ rbs})/\lambda_{LTB}$, where $r_{y\ rbs}$ is the radius of gyration about the minor axis in the most reduced section of the RBS and λ_{LTB} is the limiting value specified in design codes to avoid lateral-torsional buckling. According to AISC *Seismic provisions* (2002), λ_{LTB} is limited to $17225/F_y$ (F_y in MPa). Each of the parameters used by Uang and Fan (1999, 2001) possesses specific weak points. For instance, the influence of the RBS region vanishes in the parameter λ_{LTB} , and the flexural member becomes therefore more resistant to the lateral buckling. On the contrary, the parameter $\bar{\lambda}_{LTB}^{rbs}$ assigns the RBS properties to the whole member, and the flexural member is unintentionally weakened.

In Figs. 6(a) and (b), the rate of moment degradation due to the beam instability is plotted in terms of $\bar{\lambda}_{LTB}$ and $\bar{\lambda}_{LTB}^{rbs}$. The rate of moment degradation is defined as $M_{0.03}/M_{\max}$, where $M_{0.03}$ and M_{\max} are the maximum beam moment at the last cycle of a 0.03-radian plastic rotation, and the maximum beam moment ever developed at the column face, respectively. The definition of $M_{0.03}$ slightly differs from that introduced by Uang and Fan (1999, 2001). They considered the parameter $M_{0.03}$ as the maximum beam moment at the first cycle of a 0.03-radian plastic rotation. Since moment degradation is not the same in positive and negative bending (see Fig. 4), the more adverse state was taken as the base of evaluation of the rate of moment degradation. As it is observed in the latter figures, there is no apparent dependency between the performance of different specimens, and the results are, in fact, extremely scattered.

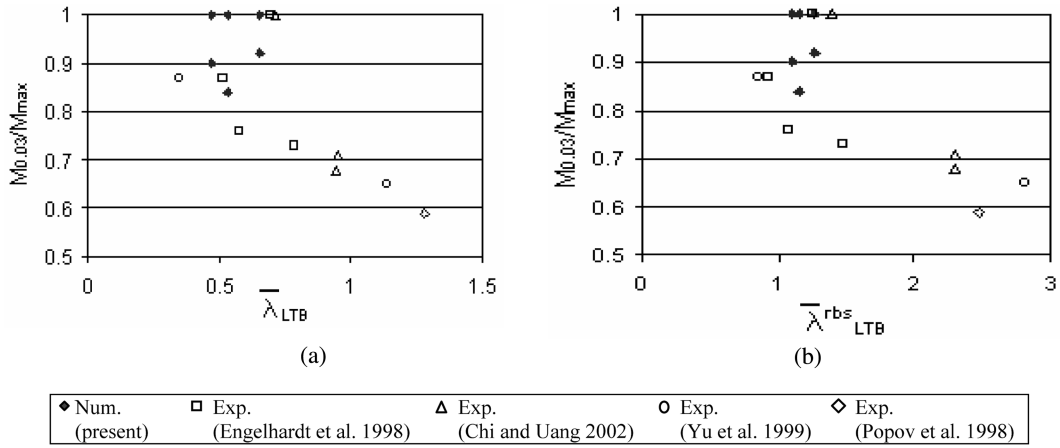


Fig. 6 Rate of moment degradation versus the lateral slenderness parameters: (a) $\bar{\lambda}_{LTB}$; (b) $\bar{\lambda}_{LTB}^{rbs}$

To discriminate the lateral instability of RBS beams from that of ordinary beams, a more convenient lateral slenderness parameter is defined in this research (see Appendix). The effect of RBS region and the effect of PZ on the lateral instability are included in this parameter, which is called *modified equivalent slenderness parameter*, $\lambda_{eq}^{modified}$.

As demonstrated in the Appendix, the lateral slenderness of a flexural member is a function of support flexibility. Modeling column panel zone as a flexible support or a rotational spring, the corresponding rotational stiffness can be expressed as follows (Krawinkler 1978):

$$\begin{aligned}
 k_{\theta e} &= \mu 0.95 d_c t_{pZ} G & \text{for } 0 \leq \gamma \leq \gamma_y \\
 k_{\theta p} &= \mu 1.095 b_{cf} t_{cf}^2 G / d_b & \text{for } \gamma_y \leq \gamma \leq 4 \gamma_y
 \end{aligned}
 \tag{4}$$

in which G , γ , γ_y are the shear modulus, the PZ shear distortion, and the shear distortion at general yielding, respectively. Factor μ equals to $1/[1/(0.95d_b) - (L_b + 0.5d_c)/(L_b H)]$, whose parameters were defined previously. For shear distortion greater than $4\gamma_y$, a constant strain hardening stiffness will describe the PZ performance.

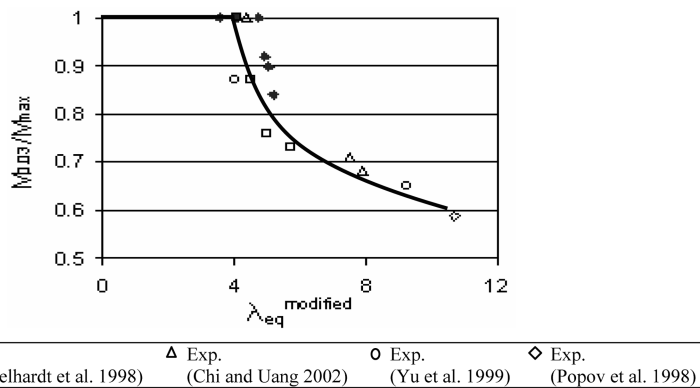


Fig. 7 Rate of moment degradation versus modified equivalent slenderness parameter

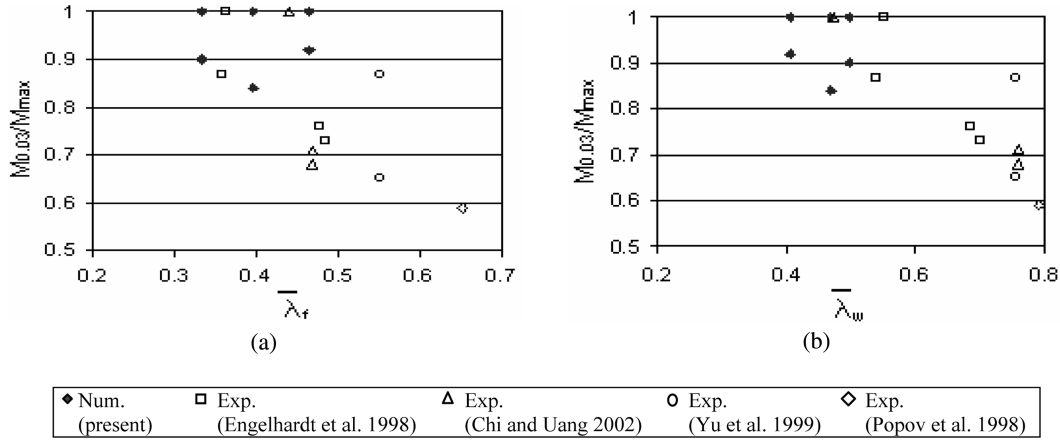


Fig. 8 Rate of moment degradation versus: (a) local flange slenderness parameter; and (b) local web slenderness parameter

The rate of moment degradation is shown versus the modified equivalent slenderness parameter $\lambda_{eq}^{modified}$ in Fig. 7. The numerical results suitably agree with the experimental data. The solid line depicted in this figure is schematically very similar to that applied by Nethercot and Trahair (1976). Comparison between Fig. 7 and Figs. 6(a) and (b) obviously demonstrates efficiency of *the modified equivalent slenderness parameter* introduced in this study.

5.2. Local buckling

The web and flange local buckling are two other sources of the instability in RBS beams. To investigate the influence of web and flange local buckling, normalized slenderness parameters (Uang and Fan 1999, 2001) are regarded as $\bar{\lambda}_f = (b_f/2t_f)/\lambda_{FLB}$ and $\bar{\lambda}_w = (h/t_w)/\lambda_{WLB}$. The parameters b_f and t_f are the beam flange width and thickness, respectively, and h is the clear distance between the beam flanges less twice fillet radius for rolled shapes. The parameters λ_{FLB} and λ_{WLB} are the limiting values specified in design codes to avoid the flange and web local buckling, respectively. Based on AISC *Seismic Provisions* (2002), λ_{FLB} and λ_{WLB} are taken as $137/\sqrt{F_y}$ and $1365/\sqrt{F_y}$ (F_y in MPa), respectively. The relation between the rate of moment degradation and the normalized slenderness parameters may be deduced from Figs. 8. No obvious correlation can be found between the local buckling modes and the rate of moment degradation.

5.3. Combined local and lateral modes of instability

To take the interaction between the local and lateral buckling modes into consideration, a nonlinear regression analysis with the following model was first carried out:

$$\lambda_e^{combined} = (\bar{\lambda}_f)^\alpha \cdot (\bar{\lambda}_w)^\beta \cdot (\bar{\lambda}_{LTB})^\gamma \quad (5)$$

where $\lambda_e^{combined}$ is the combined equivalent slenderness parameter, and exponents α , β , and γ are to be determined by regression. Each exponent implies contribution of the corresponding slenderness

parameter to the instability of an RBS beam. The parameter $\bar{\lambda}_{LTB}$ may be taken as either the parameters $\bar{\lambda}_{LTB}$ and $\bar{\lambda}_{LTB}^{rbs}$ (Uang and Fan 1999, 2001) or the parameter $\lambda_{eq}^{modified}$ which is recommended in this paper.

The regression analysis was performed by the very same procedure as used by Uang and Fan (1999) to determine the exponents α , β , and γ . The results are noted in Eqs. (6) to (8).

$$\lambda_e^{combined} = (\bar{\lambda}_f)^{0.110} \cdot (\bar{\lambda}_w)^{0.407} \cdot (\bar{\lambda}_{LTB})^{0.168} \quad (6)$$

$$\lambda_e^{combined} = (\bar{\lambda}_f)^{0.096} \cdot (\bar{\lambda}_w)^{0.388} \cdot (\bar{\lambda}_{LTB}^{rbs})^{0.177} \quad (7)$$

$$\lambda_e^{combined} = (\bar{\lambda}_f)^{0.065} \cdot (\bar{\lambda}_w)^{0.241} \cdot (\bar{\lambda}_{eq}^{modified})^{0.355} \quad (8)$$

Based on Eqs. (6) and (7), the local web buckling has the most adverse effect on the instability of an RBS beam, and the lateral-torsional and local flange buckling modes are of less importance. However, when the parameter $\lambda_{eq}^{modified}$ is regarded as a lateral slenderness index, the lateral buckling mode will become the most detrimental concern deteriorating the stability of an RBS beam.

Treating each buckling mode as an independent phenomenon for the design purposes, a linear expression, similar to that proposed by Kemp (1996), is assumed as a *combined equivalent slenderness parameter* as follow:

$$\lambda_e^{combined} = \bar{\lambda}_f \cdot \bar{\lambda}_w \cdot \lambda_{eq}^{modified} \quad (9)$$

Since the flange local buckling is of less importance in the beam instability at the required beam plastic rotation (Yu *et al.* 1999), i.e., $\theta_p = 0.03$ rad, the following expression is suggested for *the combined equivalent slenderness parameter*:

$$\lambda_e^{combined} = \bar{\lambda}_w \cdot \lambda_{eq}^{modified} \quad (10)$$

in which the effect of flange slenderness is neglected.

In Fig. 9, the rate of moment degradation is plotted versus $\lambda_e^{combined}$ based on Eqs. (6), (7), (8), and (10). The data in Figs. 9(a) and (b) is so dispersed as compared with that shown in Figs. 9(c) and (d). The authors of this paper believe that the dispersion observed in Figs. 9(a) and (b) comes from the lack of an appropriate expression for the lateral slenderness parameter. Figs. 9(c) and (d) show that the parameter $\lambda_e^{combined}$ computed by Eqs. (8) and (10) is well suited to model the instability of RBS beams. $\lambda_e^{combined}$ for experimentally and numerically tested specimens correlates well with the rate of moment degradation. The similarity between the latter figures denotes that the simple and convenient expression given in Eq. (10) provides an acceptable estimation for prediction of the beam instability occurrence. As seen in Fig. 9(d), the data is well converged to the solid trend-line drawn in the figure. Moreover, if Fig. 7 is compared with Fig. 9(d), it is interpreted that although the web buckling usually initiates the beam instability (Yu *et al.* 1999), the cyclic response of the RBS beams is mainly dominated by the lateral buckling. According to Fig. 9(d), the maximum moment deterioration may be limited to 20% providing that $\lambda_e^{combined}$ does not exceed 3, approximately.

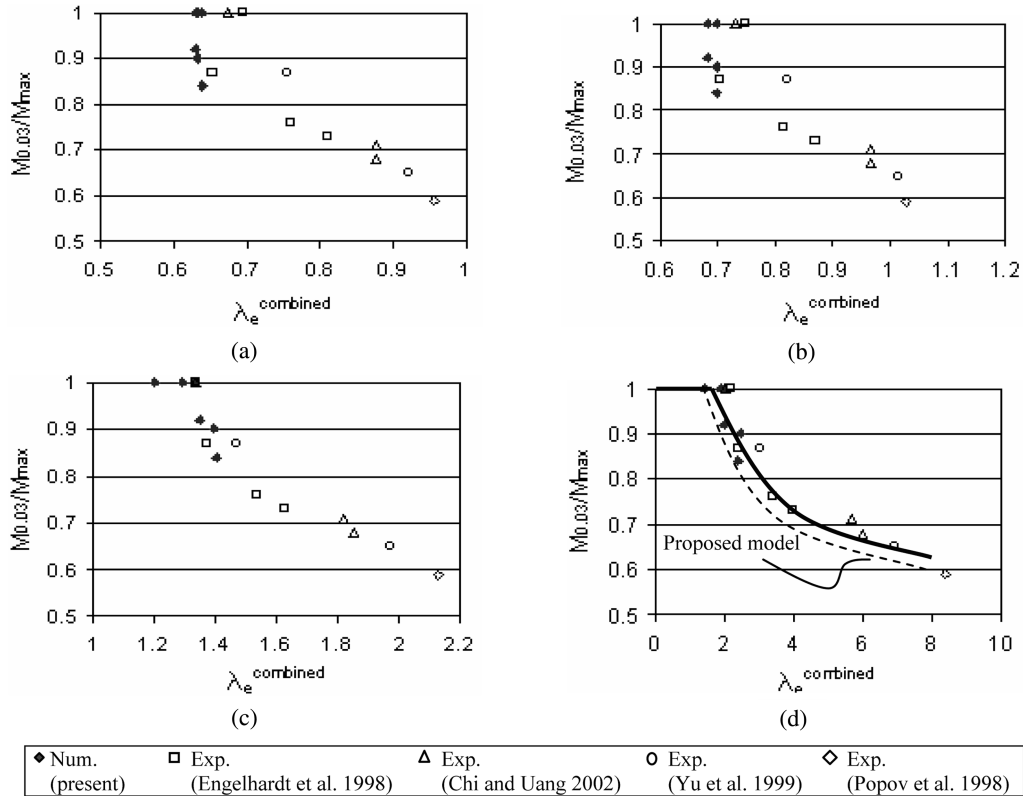


Fig. 9 Rate of moment degradation versus the combined equivalent slenderness parameter based on: (a) Eq. (6); (b) Eq. (7); (c) Eq. (8); and (d) Eq. (10)

The magnitude of $M_{0.03}$ for an arbitrary RBS beam is defined in terms of the combined equivalent slenderness parameter (obtained from Eq. (10)), and the plastic moment capacity of beam section, as follows:

$$\begin{aligned}
 M_{0.03} &= M_{\max} && \text{for } \lambda_e^{\text{combined}} \leq 1.5 \\
 M_{0.03} &= M_{\max} \left[0.5 + \frac{0.85}{\lambda_e^{\text{combined}}} - \frac{0.15}{(\lambda_e^{\text{combined}})^2} \right] && \text{for } \lambda_e^{\text{combined}} > 1.5
 \end{aligned} \quad (11)$$

In implementation, M_{\max} can be estimated by $\beta_E M_p$, where M_p is the plastic moment capacity of beam section and the coefficient β_E is limited between 0.85 and 1. As indicated in Table 4, $\beta_E = 0.85$ may be a rational initial assumption. The proposed model is illustrated in Fig. 9(d) by a dashed line. The model agrees well with the numerical and experimental data.

6. Conclusions

This paper dealt with the effects of the local and lateral slenderness as well as the effect of PZ strength on instability of RBS beams. Through a total of 19 numerical and experimental data, a model was

proposed to evaluate the magnitude of moment deterioration in terms of *the combined equivalent slenderness parameter* introduced in this study. The main results are drawn out as follows:

1. According to the evidences given in this paper, it seems that the cyclic behaviour of RBS beams is mostly dominated by the lateral-torsional buckling even though testing and this numerical study show the lateral and local modes of buckling interact each other.
2. For a column panel zone in which the ratio V_r/V_y (the design shear demand to the ultimate shear strength of PZ) is smaller than 0.7, the PZ is not expected to share with RBS region in energy dissipating.
3. In a model with strong PZ, the lateral and local buckling cause the flexural moment capacity of beam to be reduced. The amount of reduction is mainly affected by the beam lateral slenderness (Eq. (18)) and the local web slenderness. The local flange slenderness is of less significance in the moment reduction. In case of using weaker PZs the amount of moment degradation reduces.
4. According to the model proposed in this study (Eq. (10)), if the maximum moment deterioration is not to exceed 20%, a limiting value of about 3 is proposed for the combined equivalent slenderness parameter.
5. For an RBS beam with a combined equivalent slenderness parameter (Eq. (10)) less than 1.5, no reduction is likely to occur in the beam load-carrying capacity.

References

- American Institute of Steel Construction (AISC) (2002), *Seismic provisions for structural steel buildings*, Chicago.
- ANSYS (Revision 5.4) (1992), *User's Manual, Theory*, Swanson Analysis Systems, Inc, Vol. IV.
- Calado, L. (2000) "Cyclic behaviour of beam to column bare steel connection: Influence of column size", *Moment Resistant Connections of Steel Frames in Seismic Areas* (ed. Mazzolani, F. M.), E & FN SPON, 267-290.
- Chi, B. and Uang, C. M. (2002), "Cyclic response and design recommendations of RBS moment connections with deep columns", *J. Struct. Engrg.*, ASCE, **128**(4), 464-473.
- Clark, P., Frank, K., Krawinkler, H. and Shaw, R. (1997), "Protocol for fabrication, inspection, testing, and documentation of beam-column connection tests and other experimental specimens", Report No. SAC/BD-97/02, SAC Joint Venture, Sacramento, CA.
- Deylami, A. and Moslehi Tabar, A. (2004), "Effect of column panel zone characteristics on instability of beams with RBS moment resisting connections", *Proc. 13th world Conf. Earthquake Engrg.*, Vancouver, B.C., Canada, Paper No. 31.
- El-Tawil, S., Vidarsson, E., Mikesell, T. and Kunnath, S. (1999), "Inelastic behavior and design of steel panel zones", *J. Struct. Engrg.*, ASCE, **125**(2), 183-193.
- Engelhardt, M. D. and Husain, A. S. (1993), "Cyclic-loading performance of welded flange-bolted web connections", *J. Struct. Engrg.*, ASCE, **119**(12), 3537-3550.
- Engelhardt, M. D., Winneberger, T., Zekany, A. J. and Potyraj, T. J. (1996), "The dogbone connection: Part II" *Modern Steel Construction*, 46-55.
- Engelhardt, M. D., Winneberger, T., Zekany, A. J. and Potyraj, T. J. (1998), "Experimental investigation of dogbone moment connections", *Engrg. J.*, AISC, (Fourth Quarter), 128-138.
- Jones, S. L., Fry, G. T. and Engelhardt, M. D. (2002), "Experimental evaluation of cyclically loaded reduced beam section moment connections", *J. Struct. Engrg.*, ASCE, **128**(4), 441-451.
- Kemp, A. R. (1996), "Inelastic lateral and local buckling in design coeds", *J. Struct. Engrg.*, ASCE, **122**(4), 374-382.
- Krawinkler, A. (1978), "Shear in beam-column joints in seismic design of steel frames", *Engrg. J.*, AISC, **3**, 82-91.
- Mahin, S. A. (1998), "Lessons from damage to steel buildings during the Northridge earthquake" *Engrg. Struct.*,

- 20(4-6), 261-270.
- Miller, D. K. (1998), "Lessons learned from the Northridge earthquake" *Engrg. Struct.*, **20**(4-6), 249-260.
- Nethercot, D. A. and Trahair, N. S. (1976), "Inelastic lateral buckling of determinate beams", *J. Struct. Div.*, ASCE, **102**(ST4), April, 701-717.
- Plumier, A. (1997), "The dogbone: Back to the future", *Engrg. J.*, AISC, (Second Quarter), 61-67.
- Popov, E. P. (1987), "Panel zone flexibility in seismic moment joints", *Joint Flexibility in Steel Frames* (ed. W. F. Chen), Elsevier Applied Science, 91-118.
- Popov, E. P., Yang, T. S. and Chang, S. P. (1998), "Design of steel MRF connections before and after 1994 Northridge earthquake", *Engrg. Struct.*, **20**(12), 1030-1038.
- SAC (1995), "Interim Guidelines - Evaluation, repair, modification and design of welded steel moment frame structure", Report No. SAC-95-02, SAC Joint Venture.
- Trahair, N. S. and Bradford, M. A. (1988), *The Behaviour and Design of Steel Structures*, 2nd ed., Chapman & Hall, London, UK.
- Tsai, K. C. and Chen, W. Z. (2000), "Seismic response of steel reduced beam section to weak panel zone moment joints", *Behaviour of Steel Structures in Seismic Areas* (eds. Mazzolani, F. M., and Tremblay, R.), Balkema, Rotterdam, 279-286.
- Uang, C. M. and Fan, C. C. (1999), "Cyclic instability of steel moment connections with reduced beam sections", Report No. SSRP 99-21, Department of Structural Engineering, University of California, San Diego, CA.
- Uang, C. M. and Fan, C. C. (2001), "Cyclic stability criteria for steel moment connections with reduced beam section", *J. Struct. Engrg.*, ASCE, **127**(9), 1021-1027.
- Yu, Q. S., Gilton, C. and Uang, C. M. (1999), "Cyclic response of RBS moment connections: Loading sequence and lateral bracing effects", Report No. SSRP 99-13, Department of Structural Engineering, University of California, San Diego, CA.
- Yu, Q. S. and Uang, C. M. (2001), "Effects of near-fault loading and lateral bracing on the behaviour of RBS moment connections", *Steel. Compos. Struct.*, **1**(1), 145-158.

Appendix

A-1. Lateral instability

To evaluate the lateral instability of beams with RBS connections, two important issues should be clarified: (1) appropriate definition for lateral slenderness ratio, and (2) the effect of PZ flexibility on beam lateral instability. In the following, two simple but reasonable ways are presented to solve these problems.

For simplicity, it is assumed that just the compression flange resists against lateral-torsional buckling of the whole beam. As a result, beam lateral-torsional buckling is simplified to buckling of the compression flange about its strong axis. Tangent modulus E_s is assigned to the RBS region with the length of $l_{rbs} = a+b$ (see Figs. 1(b) and A1(a)). The remaining segment of the flange, l_e , is assumed to behave rigidly. Considering a constant axial force, P , the buckling equation is obtained as follow:

$$\tan(kl_{rbs}) = \frac{1}{kl_e} \quad \text{or} \quad kl_{rbs} = \tan^{-1}\left(\frac{1}{kl_e}\right) \quad (\text{A1})$$

in which $k^2 = P/E_s I_f$ and I_f = moment of inertia about the flange major axis in the RBS region. Using the following approximation

$$\tan^{-1} x \approx x \quad x \rightarrow 0 \quad (\text{A2})$$

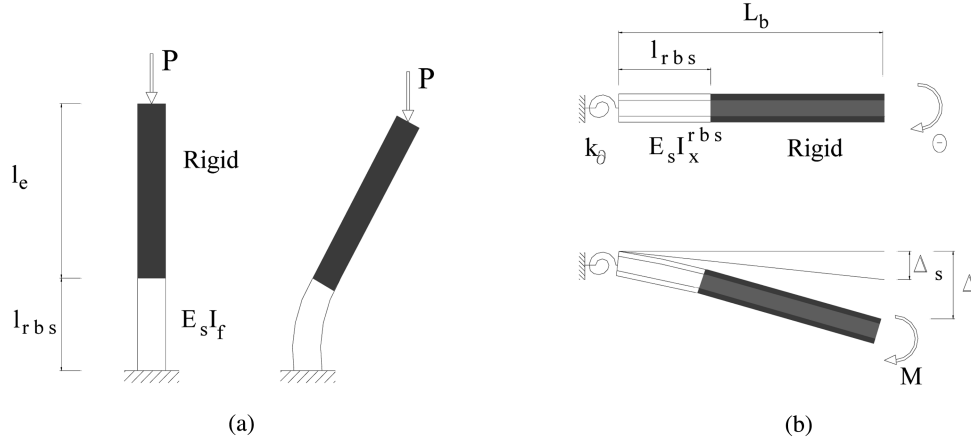


Fig. A1 (a) Buckling of compression flange; (b) flexural member connected to rotational spring

the critical load is achieved as bellow:

$$P_{cr} = \frac{E_s I_f}{l_{rbs} l_e} \quad (A3)$$

Imagine an l_{eq} long cantilever column with flexural stiffness $E_s I_f$, uniform over the whole length. For the imaginary column having the same critical load as that obtained by Eq. (A3), length l_{eq} , known as *equivalent lateral length* in this paper, must be equal to:

$$l_{eq} = \frac{\pi}{2} \sqrt{l_{rbs} l_e} \quad (A4)$$

Hence, to control if the beam with RBS connection is laterally stable, the specifications of RBS region and the equivalent lateral length, according to Eq. (A4), are taken into account.

Now, the influence of PZ flexibility should be involved in the study. To this end, consider a cantilever RBS beam connected to a rotational spring with the rotational stiffness k_θ (Fig. A1(b)). As previously assumed, tangent modulus of E_s is assigned to the RBS region with the length of l_{rbs} , and the remaining segment of the beam, l_e , is assumed to be rigid. Suppose this beam is subjected to a tip rotation, as a very simple case. The moment resulted from the beam tip rotation in terms of the induced beam tip displacement is:

$$M_b = \frac{1}{\frac{L_b}{k_\theta} + \frac{l_{rbs}(2L_b - l_{rbs})}{2E_s I_x^{rbs}}} \Delta \quad (A5)$$

in which I_x^{rbs} = moment of inertia about the beam major axis in the most reduced section. The equation represents that under the same end displacement, the moment transferred by the beam reduces as the rotational stiffness of the spring decreases. As an extreme case, the moment applied on a beam with an extremely stiff rotational spring is:

$$M_{ob} = \frac{1}{\frac{l_{rbs}(2L - l_{rbs})}{2E_s I_x^{rbs}}} \Delta \quad (\text{A6})$$

Comparing Eqs. (A5) and (A6), following relationship yields:

$$M_b = M_{ob} / \kappa; \quad \kappa = \frac{\frac{L_b + l_{rbs}(2L - l_{rbs})}{k_\theta} \frac{2E_s I_x^{rbs}}{l_{rbs}(2L - l_{rbs})}}{2E_s I_x^{rbs}} \quad (\text{A7})$$

As M_{ob} increases to its critical moment as:

$$M_e = C_b \frac{\pi}{l_{eq}} \sqrt{EI_y GJ} \sqrt{1 + \frac{\pi^2}{l_{eq}^2} \left(\frac{EI_w}{GJ} \right)} \quad (\text{A8})$$

the corresponding tip displacement reaches Δ_{cr} . In Eq. (A8), G , J , J_w , C_b = shear modulus of material, St. Venant torsional rigidity, warping rigidity, and a coefficient that allows for the moment gradient along the beam length, respectively.

But, due to a Δ_{cr} tip displacement, the beam with flexible rotational spring is still stable. Because, a portion of this displacement relates to the spring rotation (Δ_s in Fig. A1(b)), and only the reminder, which equals Δ_{cr}/κ , introduces flexural moment in the beam. Therefore, in the presence of flexible spring, the critical state is achieved when the tip displacement reaches κ times Δ_{cr} , or in other words when M_b reaches κ times the classic critical moment given in Eq. (A8), i.e.:

$$M_e^{modified} = \kappa C_b \frac{\pi}{l_{eq}} \sqrt{EI_y GJ} \sqrt{1 + \frac{\pi^2}{l_{eq}^2} \left(\frac{EI_w}{GJ} \right)} \quad (\text{A9})$$

As extensively used in design codes, the equivalent slenderness parameter $\lambda_{eq} = \sqrt{M_p / M_e}$ is prescribed in this paper with the difference that M_e is replaced by $M_e^{modified}$, as follow:

$$\lambda_e^{modified} = \sqrt{\frac{M_p}{M_e^{modified}}} \quad (\text{A10})$$

Making use of simplifying assumptions for cross-sectional properties (Trahair and Bradford 1988) in RBS region and ignoring small terms, the *modified equivalent slenderness parameter* can be approximated by:

$$\lambda_e^{modified} = \frac{1}{\pi} \frac{1}{\sqrt{\kappa} r_{y\ rbs}} \frac{l_{eq}}{\sqrt{C_b E_s}} \sqrt{\frac{F_y}{C_b E_s}}$$

where F_y , $r_{y\ rbs}$ = yield stress, and radius of gyration about the beam minor axis in the most reduced section. As given in Eq. (A7), κ is a function of rotational stiffness.

CC